



DESIGN OF A PERCOLATOR FOR AQUA-AMMONIA LIQUID

Mikdam M. Saleh Ali S. Baqir
Nuclear Engineering Department, Baghdad
University, Baghdad, Iraq

ABSTRACT

A new design concept for a percolator is developed which combine the simultaneous production of ammonia vapor plus the pumping of weak aqua ammonia liquid. The steady state design was based on a balance between the hydrostatic driving head and the total single and two-phase pressure losses in the percolator system. To accomplish this, the results from modeling of the driving pressure and pressure losses, using the separated flow and drift flux methods were compared with the experimental measurements. The Chisholm's model was the best in predicting the measured flow rate versus water level for first stage with a maximum standard deviation of $\pm 10.1\%$ and was adopted for the theoretical calculations. Parametric design studies that include the cooling power and the strong solution level, inner tube diameter and height for each stage of the percolator were carried out to maximize suitable cost function. The results of the optimization gave a two stage percolator of length 280 mm, inner diameter 5.5 mm for first stage and length 520 mm, inner diameter 5.5 mm for second stage.

الخلاصة

تم تطوير فكرة تصميم جديد لمبخر نفاث والذي يجمع بين انتاج بخار الامونيا وعملية الضخ لسائل امونيا ضعيف التركيز. ان تصميم الحالة الثابتة قام على اساس التوازن بين القوة الدافعة الهيدروستاتية وبين فقدان الضغط الناجم عن الجريان الاحادي والثنائي الطور في نظام المبخر. لغرض اتمام ذلك فإن النتائج المستحصلة من عملية تمثيل للضغط الدافع وكذلك فقدان الضغط باستخدام الجريان المنفصل والجريان المنبثق الانحرافي تم مقارنة الحسابات النظرية بالقياسات العملية باستخدام الماء كسائل العمل. لتحديد الموديل المناسب لفقدان الضغط تبين أن (موديل جزم) يعتبر الافضل في التنبؤ بقياسات معدل الجريان مقابل مستوى الماء بالنسبة للمرحلة الاولى حيث إن الانحراف المعياري كان $\pm 10.1\%$. إن استخدام التصميم البارامتري (الذي يشمل على طاقة التبريد، مستوى المحلول القوي، قطر الانبوب الداخلي وارتفاع كل مرحلة بالنسبة للمبخر) توصل الى إيجاد الابعاد المثلى للمبخر والمتمثلة بمبخر ذو مرحلتين بطول 280 ملم وبقطر 5.5 ملم بالنسبة للمرحلة الاولى ويطول قدره 520 ملم وقطر داخلي 5.5 ملم بالنسبة للمرحلة الثانية .

KEY WORDS

Percolator, pressure drop, natural circulation and Bubble pump

INTRODUCTION

Information on percolator or bubble pump design, also known as vapor-lift pump, is sparse in the open literature. Percolating coffee makers are a well-known application of bubble pumps. Heat addition to the fluid at the base of a vertical tube creates vapor, thereby increasing the buoyancy of the fluid causing it to rise through the vertical tube under two-phase flow conditions.

Air-lift pumps run on the same principal as vapor-lift pump except that air is injected to increase the buoyancy of the fluid instead of bubbles forming from liquid vaporization.

Delano, A. D. 1998, and Schaefer, L. A. 2000, designed a model, based on the air-lift pump analysis of Stenning and Martin, 1968, and analyzed the performance of the bubble pump, using energy balance for an idealized Einstein cycle.

Recently there has been a lot of interest in the Platen and Munters cycle. Herold et. Al, 1996 gave a review of the details of its operation and performance. Chen et al, 1996 investigated the diffusion-absorption cycle for enhancing its performance.

More recently, Sathc, 2001-used Delano's methodology applied to the Platen-Munters bubble pump, built and tested the bubble pump.

The working fluid used was methyl alcohol (methanol). Methyl alcohol has a boiling point of 64 °C. The bubble pump was tested extensively for varying heat inputs, different pump tube diameters and driving heads at constant ambient pressure. The influence of these parameters on the flow rate of the pumped liquid were discussed in detail.

This percolator is to be designed as part of a domestic absorption refrigerator with a cooling load/capacity of 200 W (Saleh, M. M. 2000). Previous design concepts combine the boiler unit responsible for the production of ammonia vapor with a separate air/vapor pump unit to effect pumping of the weak aqua ammonia solution. In this work new concept will be developed for the simultaneous production of ammonia vapor and pumping of weak aqua ammonia in a single unit.

The design will be based on the mass, concentration and energy balance the discretised elements of the percolator and to calculate the driving pressure and pressure losses, using separated and drift flux models. An experimental percolator will be built and operated to compare the different calculation models in order to select the most appropriate. Finally a parametric optimization procedure will be adopted to find the optimum geometry and dimensions of the percolator.

Theoretical Modeling

The percolator in Fig. (1) is driven by natural circulation, which is effected by a suitable designed strong solution level, diameter and length of percolator tubes to provide an optimum flow rate ratio. The percolator consists of two stages, the first stage receives a slightly subcooled strong solution from the reservoir unit which was passed through a double tube heat exchanger to reclaim heat from the weak solution flow to the absorber unit. The other stages receive saturated solution that is dictated by system pressure and inlet solution temperature. It should be noted that boiling does not occur at a single temperature but at progressively higher temperatures as the concentration through the percolator decreases. This temperature glide is due to the ammonia water solution being zeotropic.

A boiling fluid in a flow system encounters several resistances to flow, manifesting themselves in pressure drops. Two of largest are due to friction and acceleration as the fluid undergoes an increase in volume as it receives heat from the channel. Other pressure drops are due to abrupt changes in flow area such as at exits and entrances.

The heat flux is assumed to be constant along the heated section of length L , and this can be accomplished by wrapping the heated section by glass wool insulation. This arrangement tends to reduce the temperature gradient along the heated section. The heat received by the first stage of length L_1 for example may be evaluated as:

$$q_1 = \frac{L_1}{\sum_{j=1}^N L_j} Q \tag{1}$$

Where Q = total heat supplied to percolator and N = number of stages.

In designing a natural circulation percolator, it is especially important that all possible pressure changes should be evaluated as accurately as possible.

In Fig. (1) define L_o as the non-boiling height (i.e only sensible heat is added to the incoming subcooled solution. At $z = L_o$, the coolant becomes saturated. The remainder of the channel is that in which boiling takes place and is called the boiling height, L_B . Some subcooled boiling may, of course, occur in L_o but will have little effect on pressure drops or density. The ratio L_o/L_1 may be evaluated from the ratio of sensible heat added to total heat added thus:

$$\frac{L_o}{L_1} = \frac{h_L - h_w}{h_L + x_e h_{LV} - h_w} \tag{2}$$

Where x_e is the exit quality from the channel and h_L, h_{LV}, h_w are the saturated enthalpy, latent heat of vaporization at the average stage concentration and enthalpy of subcooled inlet solution respectively.

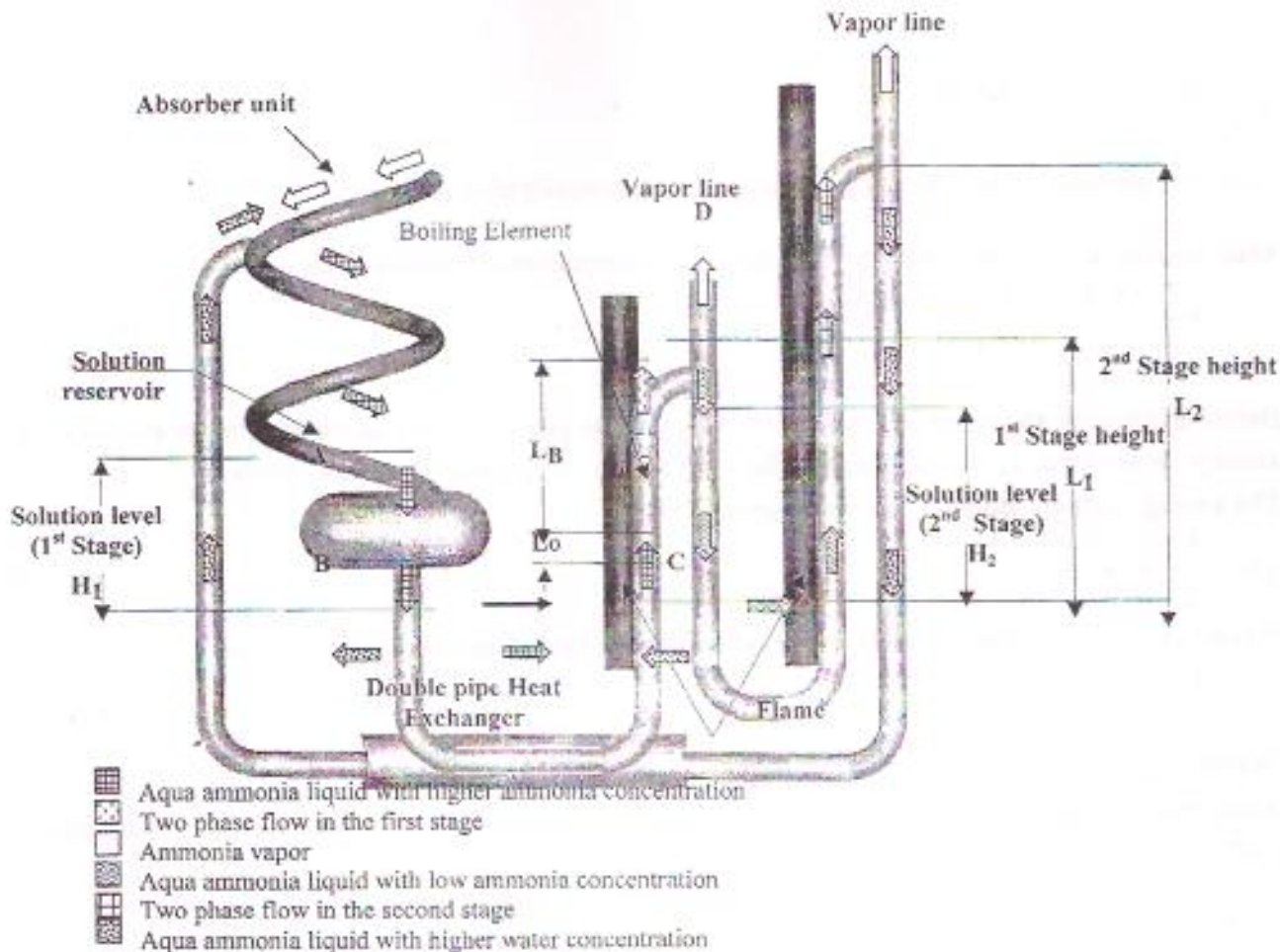


Fig. (1): A simple schematic diagram of a percolator showing stages.

Performing an energy balance for a differential element as shown in figure 1, the exit quality from the element may be written as:

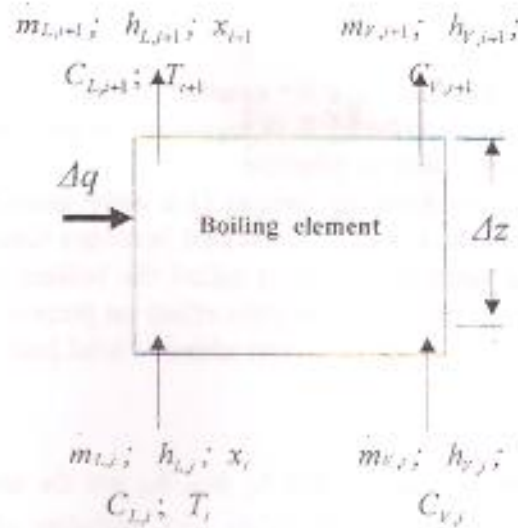


Fig. (2) differential boiling element analysis

$$x_{j+1} = \frac{h_{L,j} + x_j h_{LV,j} + \Delta q / m_w - h_{L,j+1}}{h_{LV,j+1}} \quad (3)$$

Note: All enthalpies are a function of the ammonia concentration C .

Mass balance for boiling element gives the exit concentration of ammonia as:

$$C_{L,j+1} = \frac{(1-x_j)C_{L,j} + x_j C_{V,j} - x_{j+1} C_{V,j+1}}{(1-x_{j+1})} \quad (4)$$

Before evaluating the water level H for the stage of the percolator, its necessary first to evaluate the average densities in L_o , L_B and through the inlet supply ρ_o , ρ_B and ρ_m respectively.

The average density along L_o may be evaluated from:

$$\rho_o = \frac{1}{2}(\rho_i + \rho_L) \quad (5)$$

Where ρ_i , ρ_L are densities at the inlet and exit to the heated section. And similarly:

$$\rho_w = \frac{1}{2}(\rho_{res} + \rho_i) \quad (6)$$

Where ρ_{res} = liquid density at the reservoir.

While the average density along the boiling channel, ρ_B for uniform heat flux was shown by Baqir, 2002:

$$\rho_B = \rho_i - (\rho_L - \rho_V) \frac{1}{1-\varphi} \left\{ 1 + \left[\frac{1}{\alpha_c(1-\varphi)} - 1 \right] \ln(1 - \alpha_c(1-\varphi)) \right\} \quad (7)$$

Where



$\phi = \frac{\rho_v}{\rho_l} S$, and ρ_v is the saturated density of the vapor mixture at average temperature of the element. The friction pressure drop along the single phase path (refer to figure 1) may be evaluated by the Darcy formula given below:

$$\Delta p_f = f \frac{L}{2D} \rho V^2 \quad (8)$$

f = Darcy-Weisbach friction factor = four times f Fanning.

= $64/Re$ for laminar flow.

= $0.184/Re^{0.2}$ for turbulent low [El-Wakil].

The two-phase friction pressure drop ΔP_{TP} is given by El-Wakil, 1979 :

$$\Delta p_{TP} = f \frac{1}{2D} \frac{m^2}{\rho_l} [(1-x)^{1.75} \phi_l^2 tt] \quad (9)$$

Where;

$\phi_l^2 tt$ = Martinelli-Nelson friction pressure drop multiplier.

Chisholm, 1972 expressed $\phi_l^2 tt$ as:

$$\phi_l^2 tt = [1 + (\Gamma^2 - 1)(Bx^9(1-x^9) + 1.8x)] / (1-x^{1.75}) \quad (10)$$

Where:

$$\Gamma = \left(\frac{\rho_l}{\rho_v} \right)^{0.5} \left(\frac{\mu_v}{\mu_l} \right)^{0.1} \quad (11)$$

And B is a parameter that depends on Γ and G as given by table 1.

Because the solution undergoes an increase in volume as it receives heat in a boiling channel, it accelerates as it travels through the channel. An acceleration pressure drop may be evaluated from a relationship involving the change in momentum of the incoming and outgoing solution. Collier, 1996 gave the equation for acceleration pressure drop in a boiling channel as:

$$\Delta p_a = G^2 \left[\frac{(1-x_e)^2}{\rho_l(1-\alpha_e)} + \frac{x_e^2}{\alpha_e \rho_v} - \frac{1}{\rho_v} \right] \quad (12)$$

Where;

Δp_a = pressure drop due to acceleration.

G = total mass flow rate per unit cross-sectional area of the boiling channel.

Because of the density differential between regions A-B & C-D (see figure 1), then a driving pressure will exist and cause a flow in the direction indicated. The driving pressure can be written as ;

$$\Delta p_d = g[\rho_{in}H - (\rho_o L_o + \rho_B L_B + \rho_V L_V)] \quad (13)$$

Where;

Δp_d = driving pressure

At steady-state, the driving pressure must equal the total system losses along the stage. This is expressed as:

$$\sum \Delta P_d = \sum \Delta P_f + \sum \Delta P_a + \sum \Delta P_{mm} \quad (14)$$

Where;

$\sum \Delta P_f$ = sum over the elements of friction pressure losses(in inlet line, heated and vapor line.

$\sum \Delta P_a$ = sum over the elements of the acceleration pressure drop through L_B .

$\sum \Delta P_{mm}$ = sum over the elements of the minor losses (As based on the development by El-Wakil.

There are many correlations to calculate the void fraction such as the separated flow and drift flux flow models. In the separated flow model, Chisholm formulated the following equation to evaluate the void fraction α :

$$\alpha = 1 - \frac{1}{\sqrt{\phi^2 / u}} \quad (15)$$

Table (1) parameter B in Chisholm's equation.

Γ	$G, \text{kg/m}^2\text{s}$	B
≤ 9.5	≤ 500	4.8
	$500 < G < 1900$	$2400/G$
	≥ 1900	$55/G^{0.5}$
$9.5 < \Gamma < 28$	≤ 600	$520/(\Gamma G^{0.5})$
	> 600	$21/\Gamma$
> 28	-----	$15000/(\Gamma^2 G^{0.5})$

The drift flux model, formalized by Zuber and Findlay, 1965, provides a means to account for the effects of the local relative velocity between the phases. It relates the average vapor void fraction of two-phase flow to: 1) the superficial velocities (the velocity each phase would have if they occupied the entire area of the pipe alone) of the vapor and liquid phases; 2) C_o , the distribution parameter; and 3) V_{gj} ($= V_V - j$), the drift velocity. The resulting drift model can be summarized by the following equation:

$$\alpha = \frac{j_V}{C_o(j_L + j_V) + V_{gj}} \quad (16)$$

Where j_L and j_V are defined as;

$$j_L = m_{in} (1-\alpha) / (A_i \rho_L)$$

$$j_V = m_{in} \alpha / (A_i \rho_V)$$

Where,

m_{in} = inlet mass flow rate to the Percolator.

D_i = inside diameter of the boiling channel.

Many authors have formulated empirical correlations for C_o and V_{gj} depending on the two-phase vertical flow regimes. In the current study, four models were examined which used different representations for C_o and V_{gj} as described below:

**Nicklin Correlation**

Nicklin et al., 1962 formulated the following equations for the drift velocity:

$$C_o = 1.2$$

$$V_{gj} = 0.35 \sqrt{\frac{g(\rho_L - \rho_V)D}{\rho_L}} \quad (17)$$

Reinemann Correlation

Reinemann et al., 1990 attempted to take into account surface tension effects σ by altering the V_{gj} term:

$$V_{gj} = 0.352(1 - 3.18\Omega - 14.77\Omega^2) \sqrt{gD} \quad (18)$$

Where,

The surface tension number is given by

$$\Omega = \frac{\sigma}{\rho g D^2}$$

De Cachard & Delhave Correlation

De Cachard and Delhave, 1996 took surface tension effect into account and came up with an alternative empirical correlation for the V_{gj} term:

$$V_{gj} = 0.345 \left(1 - e^{-0.01 N_f / 0.345} \right) \left[1 - e^{(3.37 - B_o) / m} \right] \sqrt{gD} \quad (19)$$

Where,

$$(N_f)^2 = \frac{\rho_L (\rho_L - \rho_V) g D^3}{\mu_L^2} \quad (20)$$

$$B_o = \frac{(\rho_L - \rho_V) g D^2}{\sigma} \quad \text{which is called the Bond number}$$

And m is defined for different ranges of N_f by the following table:

N_f	m
> 250	1
$18 < N_f < 250$	$69 (N_f)^{-0.35}$
< 18	25

Delano Correlation

Finally, the correlation of Delano, 1998, arrived at the following relation for the void fraction:

$$\alpha = \frac{1}{1 + S \frac{j_L}{j_V}} \quad (21)$$

Where,

$$S = \text{slip ratio} = \frac{V_V}{V_L} \quad (22)$$

Experimental Setup

The goal from the experimental setup is to compare the theoretical calculations from the above models that deals with evaluating α and choose a model that predict the experimental results with the highest accuracy.

The experimental percolator depicted in Fig. (3) is a two stage no recirculation type, the 1st stage consist of two identical tubes of length 280 mm each, and the 2nd stage has a single tube of length 520 mm, the inner diameter for all tubes is equal to 5.5 mm with 1 mm wall thickness. The first stage receives a slightly subcooled liquid from the reservoir through the annulus of a double pipe heat exchanger with 2.75 m length, the outer diameter for the inner pipe is 9 mm with 2 mm thickness and the outer diameter for the outer pipe is 15 mm with 1 mm thickness. The two stages are welded to a heat distribution pipe of the system which is also used as a chimney (1.15 m length) to carry out the flue gases out, The percolator is made from 304L stainless steel.

Several modified models based on the separated and drift-flux flow models were used to calculate the water mass flow rates for different water levels. The theoretical calculations from these models are compared with the experimental results in Fig. (4) in order to choose the most suitable model. It can be seen that the Chisholm model gave the best prediction to the experimental results (with a maximum error of 10 %) and consequently was adopted for the theoretical calculations. This conclusion agrees with the standard deviation estimate presented in Table (2) for several models.

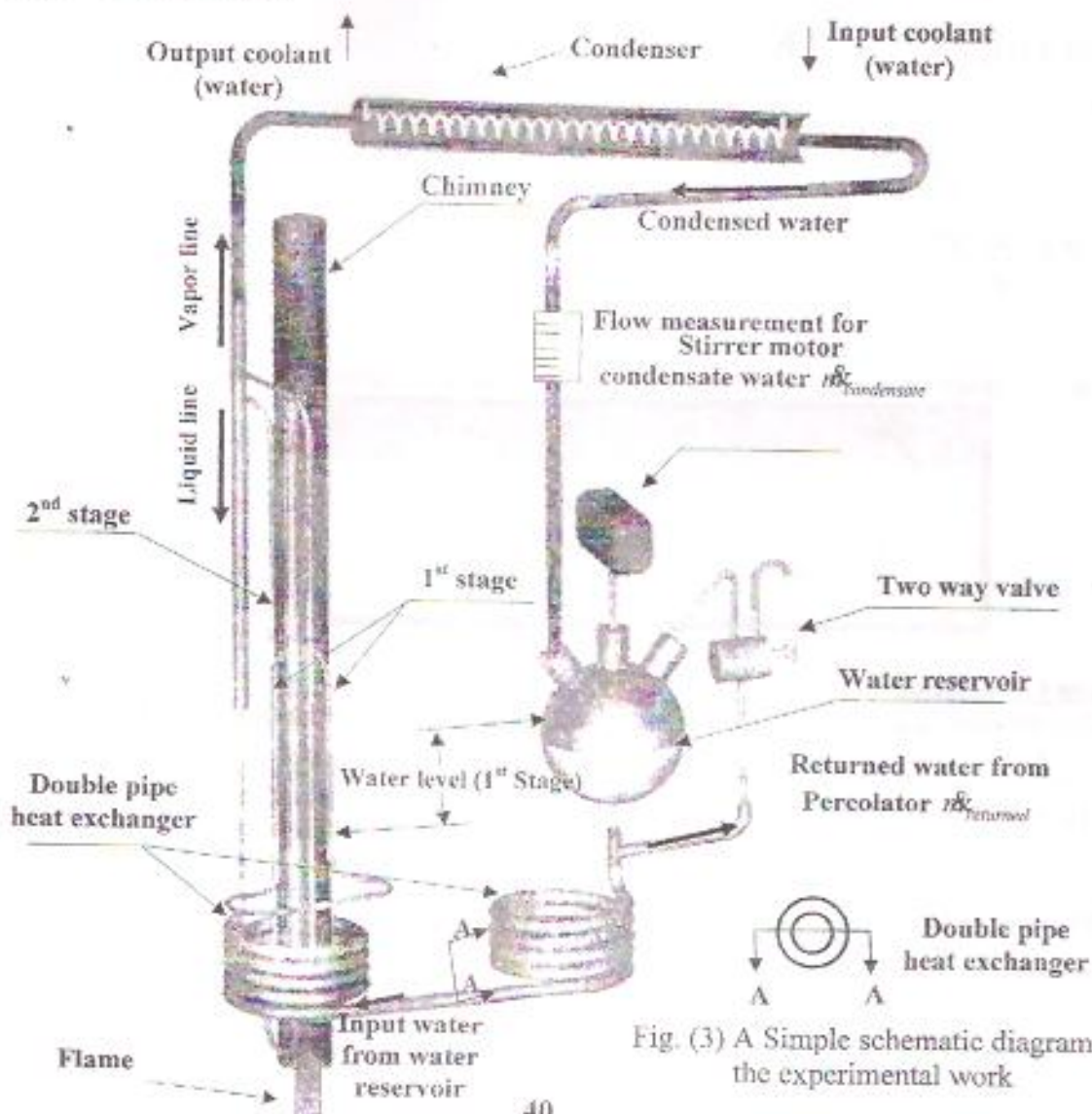


Fig. (3) A Simple schematic diagram of the experimental work



Table (2) Percent standard deviation σ for input mass flow rate*

Type of correlation	Chisholm	Delano	Nicklin	Rienemann	de Cachard
Standard deviation	10.10%	29.3%	27.4%	37.35%	31.98%

$$* \sigma = \sqrt{\frac{1}{n-1} \sum_{i=1}^n \left(\frac{\dot{m}_{model} - \dot{m}_{exp.}}{\dot{m}_{model}} \right)^2}$$

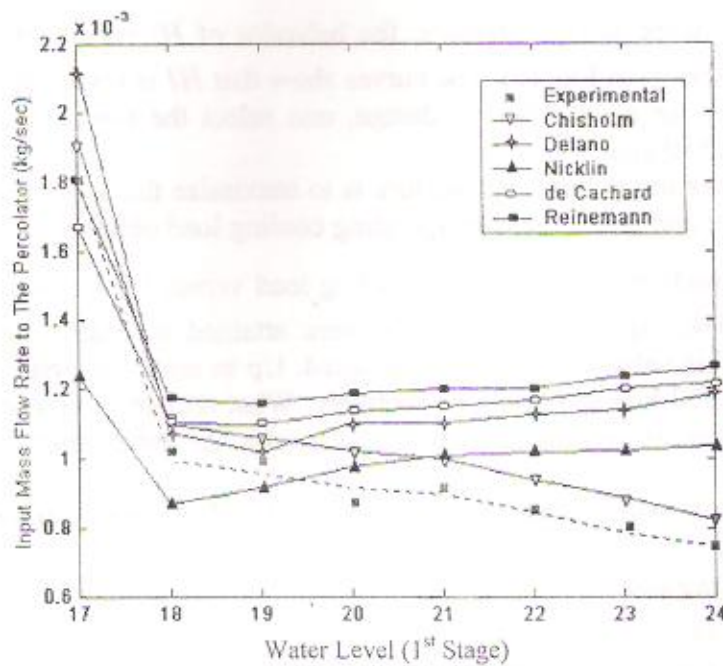


Fig. (4) Input mass flow rates vs. 1st stage water level

Results and Discussions

Before presenting the results, it should be borne in mind that the space allocated to the percolator is subjected to limitations which are summarized in Table (3) below along with other constraints: (Saleh, 2000)

Table (3) Design limitations;

Maximum height allocated	580 mm
Maximum width allocated	150 mm
Maximum strong solution level H ₁ H ₂	160 mm ≤ L ₁
Cooling load	200 w
Operating range for System's pressure	(1530-1800) kpa

The process of designing the percolator can be divided into the following consecutive steps; where each step is evaluated separately and the first step to satisfy the design requirements will be implemented:

- 1- One tube percolator (one stage).
- 2- One tube for each the first and second stage (single tube/two stage).
- 3- Two tubes for first stage and one tube for second stage (two tube first stage).

For the first and the second steps the calculated required level, H is much greater than the maximum H of 160 mm. Clearly, these arrangements cannot be used. For step(3), the strong solution level for first stage is lower than the maximum limit of 160 mm for all the inner tube diameters considered as in Fig. (5).

The system's parameters of interest are: system pressure P , inner tube diameter D_i , height for each stage, L_1 and L_2 , strong solution levels for first and second stage, H_1 and H_2 and the ammonia vapor fraction VF .

In order to select the worst design pressure, the behavior of H_1 versus m_{in} for various possible system pressures are shown in Fig. (6). The curves show that H_1 is inversely proportional to system pressure P . Therefore, for a conservative design, one select the lowest possible system pressure which correspond to 1530 kpa.

An important parameter in the design procedure is to maximize the ammonia vapor flow rate for a given input heat power and hence the corresponding cooling load obtained in the evaporator.

Attention is now focused on the behavior of cooling load versus VF for two values of m_{in} . This is shown in Fig. (7). The highest cooling loads were attained at nearly the same vapor fraction ($VF=0.575$). Hence, this value of VF will be adopted. Up to now, the system's pressure and vapor fraction are fixed at 1530 kpa and 0.575 respectively. What remain to be considered are L_1 , L_2 , H_1 and D_i . The behavior of cooling load L_1 , L_2 , H_1 with the tube inner diameter are shown in Fig. (8).

A suitable cost function, which maximizes cooling load and minimizes dimensions of the system can be defined as:

$$\text{Cost Function} = \frac{\text{Cooling Load}}{(H_1)(L_1)(L_2)}$$

The cost function is shown in Fig. (9) which indicates the presence of an optimum at a diameter of $D_i=5.5$ mm. This diameter corresponds to tube length of $L_1=280$ mm for the first stage and $L_2=520$ mm for the second stage. For This optimum design configuration, Figs. (10 to 13) shows the temperature/ammonia concentration along the first and second stage respectively.

Fig. (10) shows the monotonic increase in temperature of the first stage with the obvious implication that the boiling temperature along the tube rises continuously as the corresponding concentration becomes more depleted in ammonia. This phenomenon is referred to as temperature glide, normally associated with zeotropic solutions. Figs (12) and (13) show the profiles of the frictional, acceleration and total pressure losses along the first and second stage respectively.

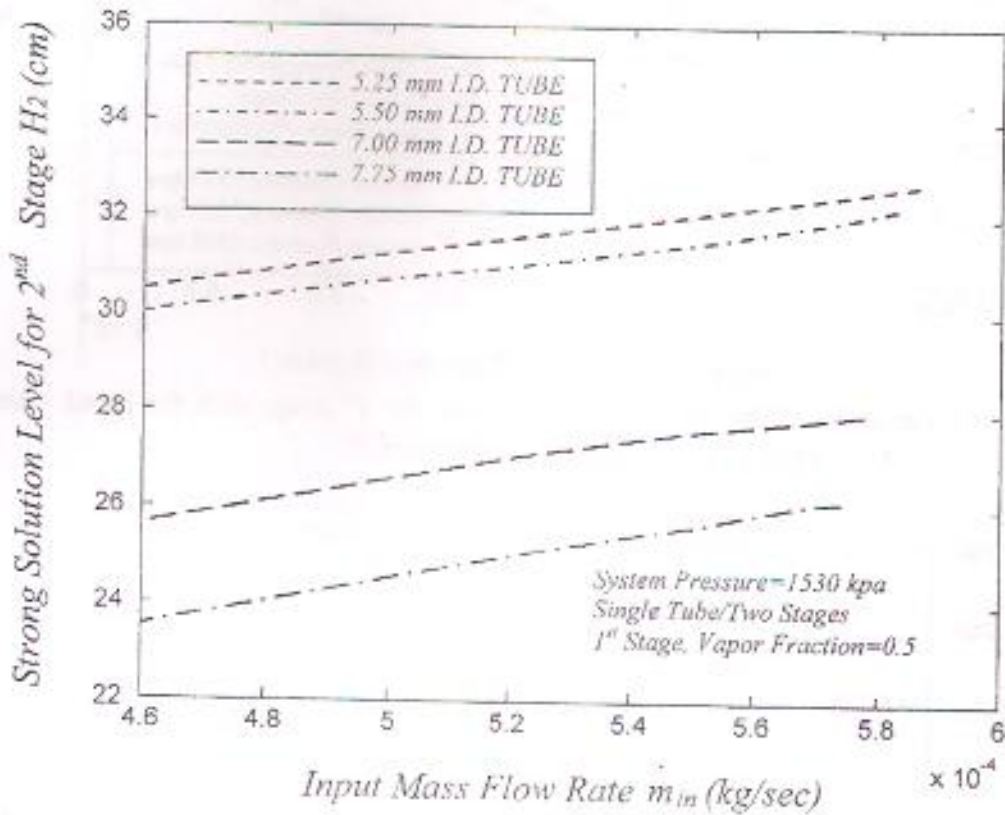
These profiles shows the slopes to increase monotonically due to the subsequent rise in both the quality and void fraction of the two phase flow along the stages.

A final observation in regard to the average water content in the exit ammonia water vapor mixture is in order. It is to be expected that in a multi stage design, owing to temperature glide, each successive stage generates a higher water vapor content than its preceding stage. This in effect indicates that the higher the number of stages, the lower the average water content at the exit. This observation is confirmed in Table (4) below, which relates the average water vapor content with the number of stages.



Table (4) Average concentration of water in vapor mixture with the number of stages.

Number of stages	1	2	3
Average concentration of water in vapor mixture	0.209	0.2	0.191

Fig. (5) Variation of the Strong Solution Level for 2nd Stage with the Input mass flow rate for Single Tube/Two Stages as a function of D_t .

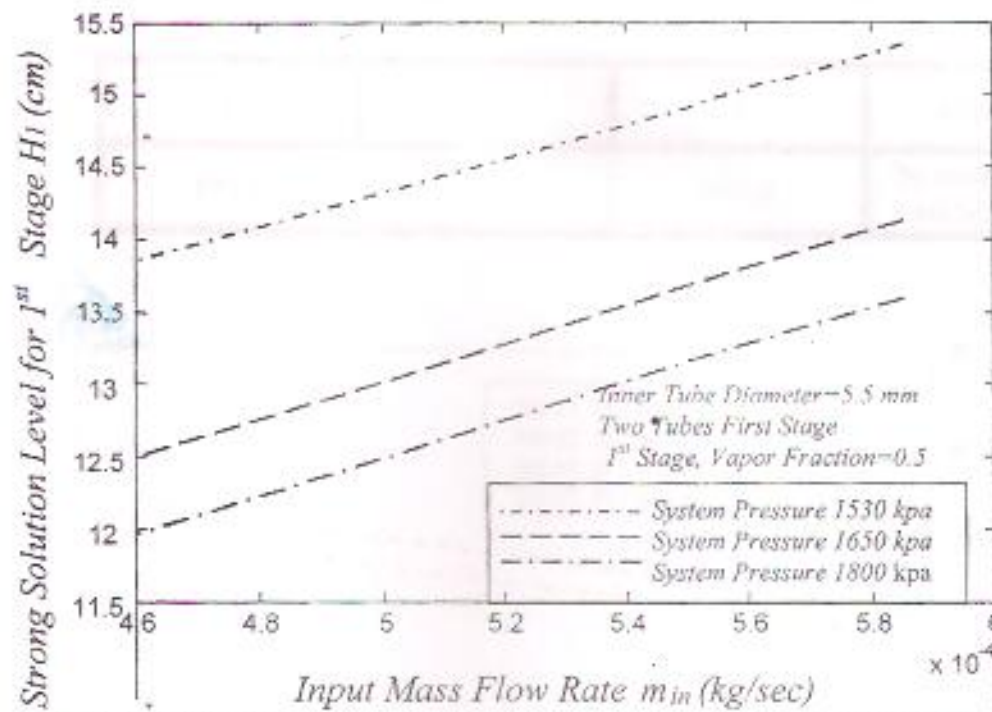


Fig. (6) Variation of the Strong Solution Level for 1st Stage with the Input mass flow rate as a function of system pressure P .

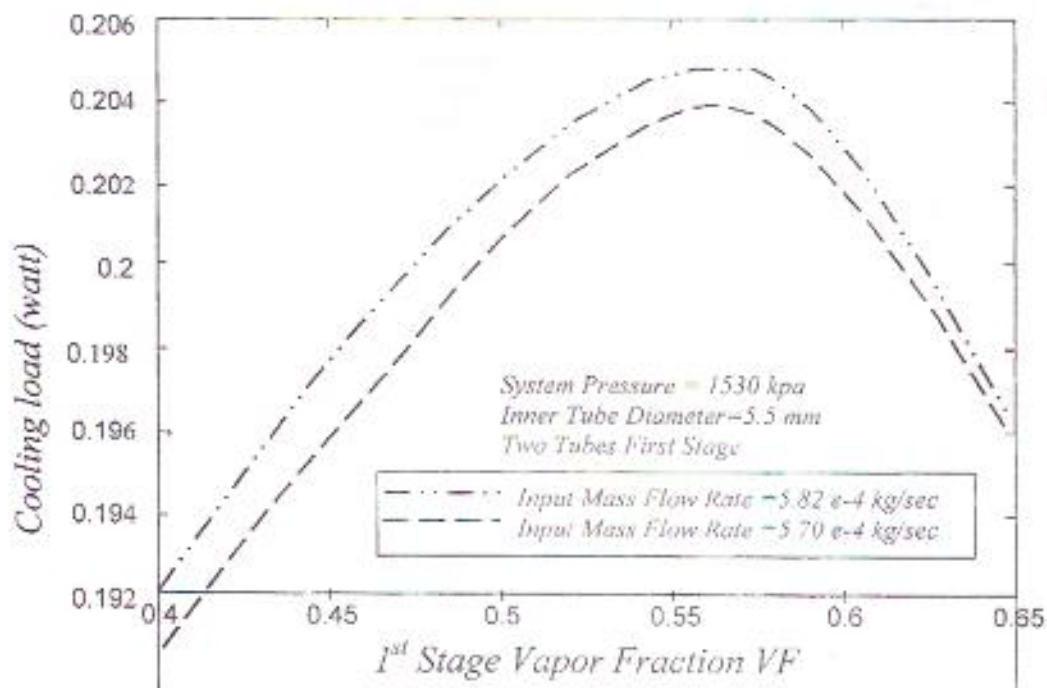


Fig. (7) Variation of the Cooling load with the 1st Stage Vapor Fraction VF .

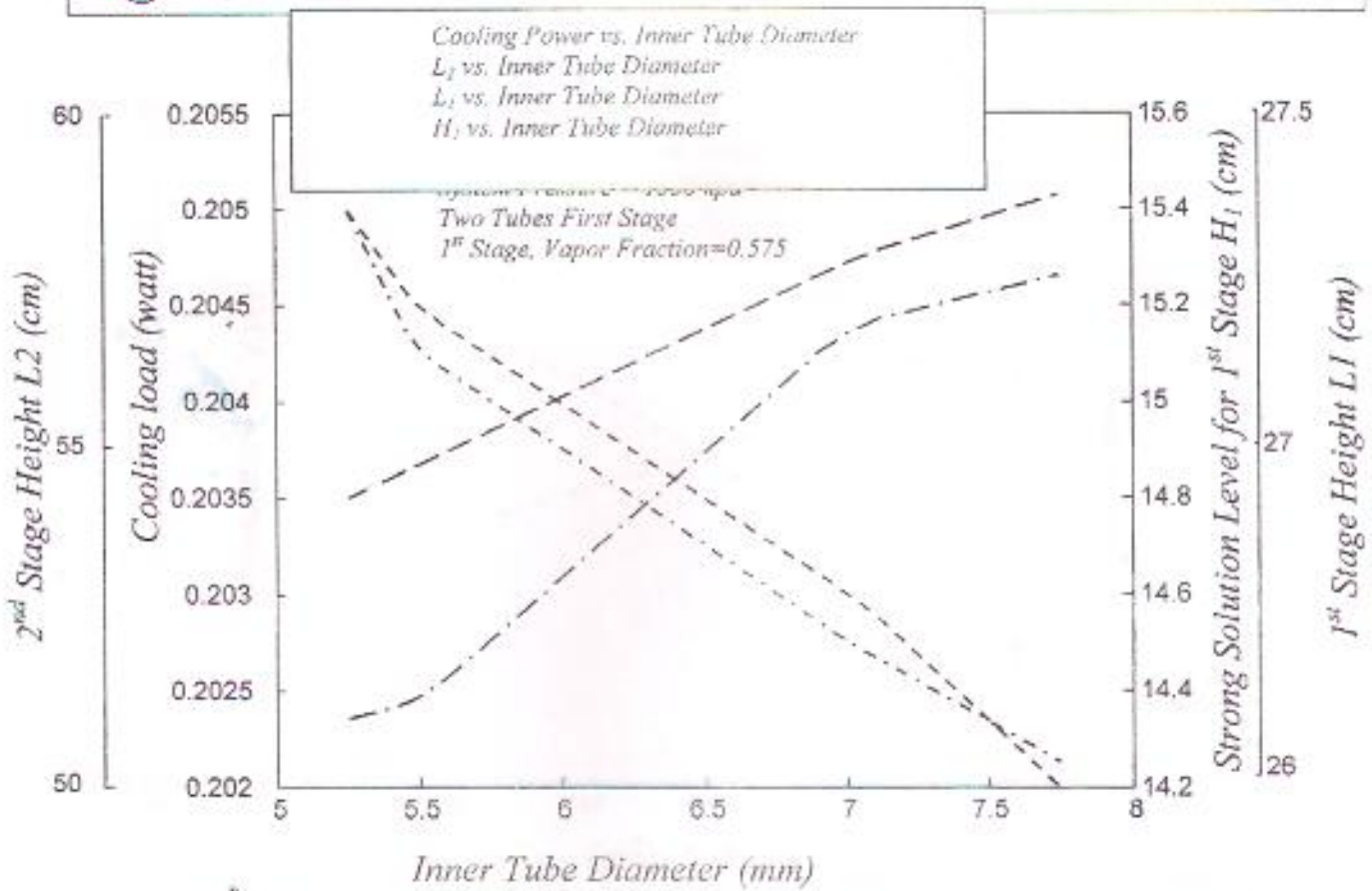


Fig. (8) Variations of the Cooling load, L_1 , L_2 and H_1 with the Inner Tube Diameter D_i .

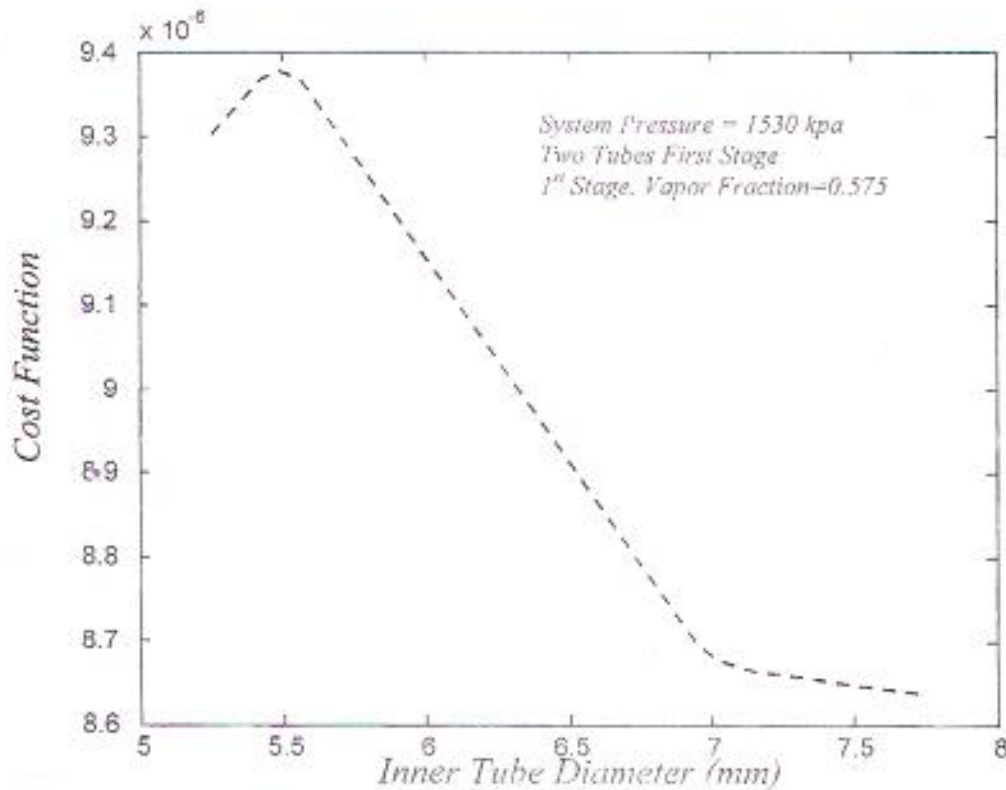


Fig. (9) Variations of Cost Function with the Inner Tube Diameter D_i .

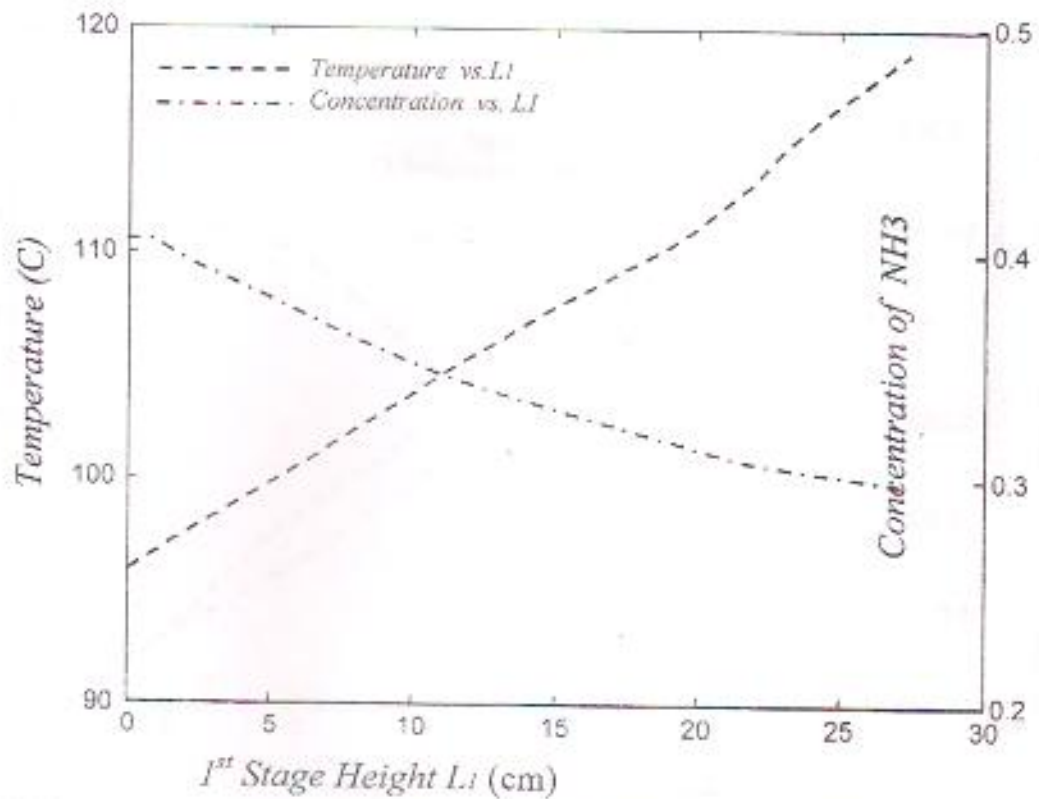


Fig. (10) Variations of the Temperature and Concentration with the 1st Stage Height L₁.

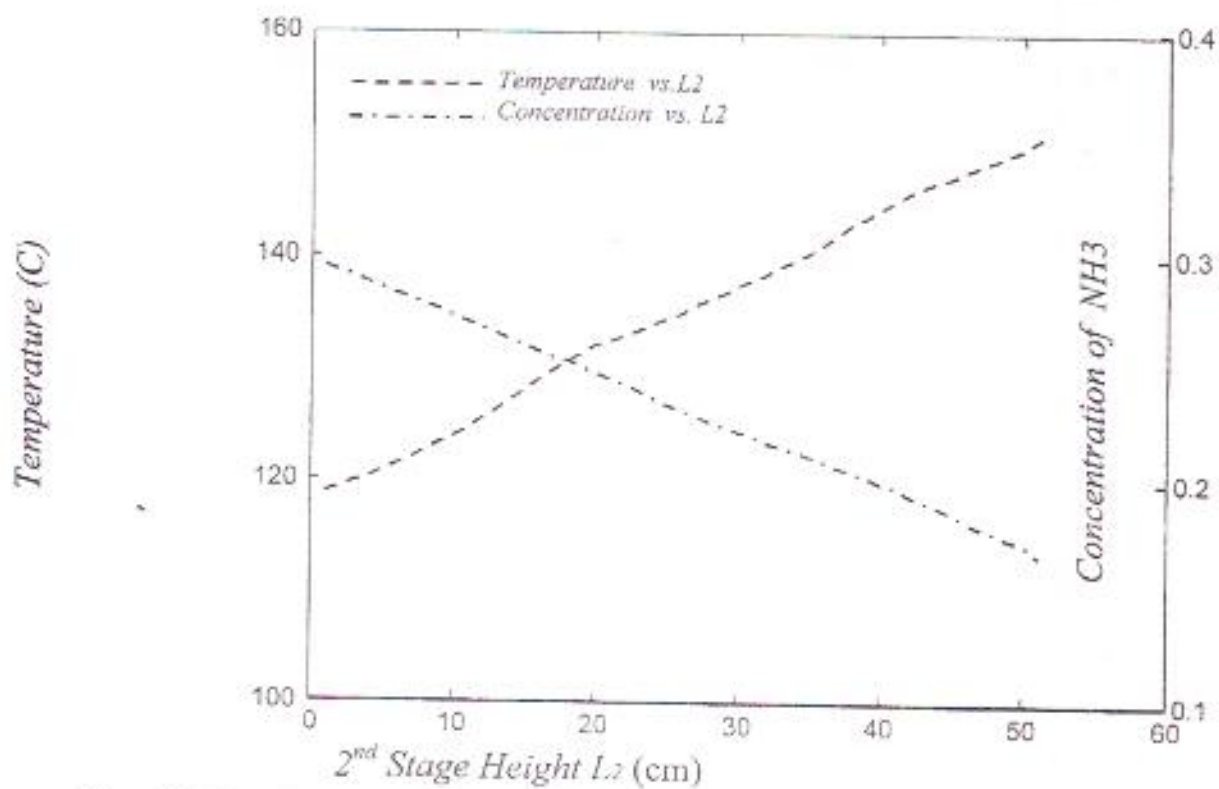


Fig. (11) Variations of the Temperature and Concentration with the 2nd Stage Height L₂.

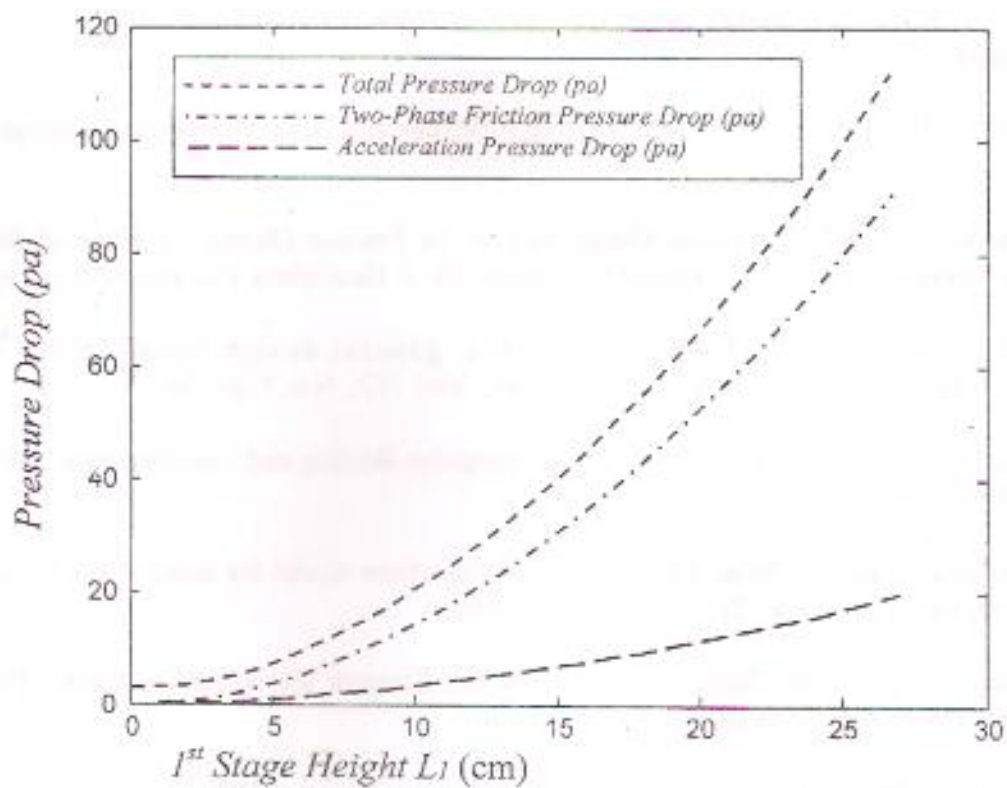


Fig. (12) Variations of Acceleration, Two-Phase Friction, and Total Pressure Drop with the 1st Stage Height L_1 .

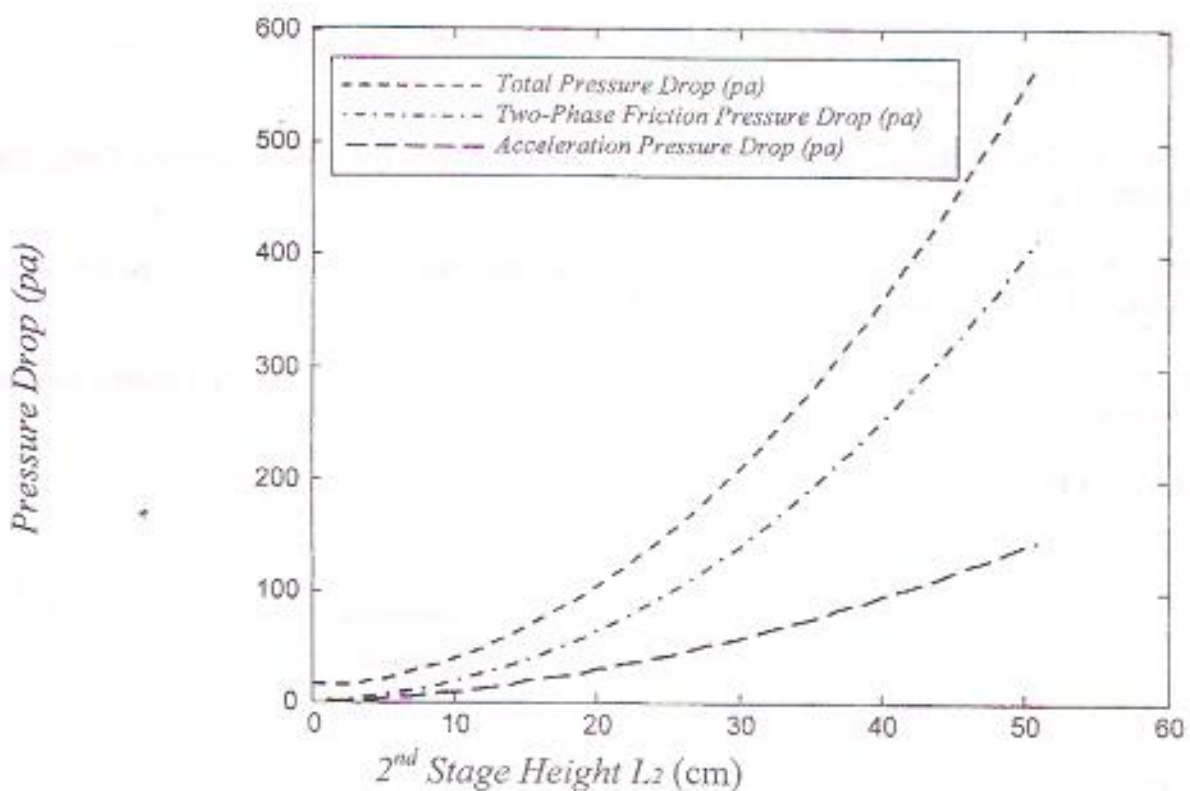


Fig. (13) Variations of Acceleration, Two-Phase Friction, and Total Pressure Drop with the 2nd Stage Height L_2 .

REFERENCES

- Baqir, A. S., (2002), Design of A Percolator for Aqua-Ammonia Liquid, M. Sc. Thesis, University of Baghdad,.
- Chisholm, D., (1983), Two-Phase Flow in Pipelines and Heat Exchangers, George Goodwin, New York.
- Chisholm, D., (1972), Pressure Gradients Due To Friction During the Flow of Evaporating Two-phase Mixtures in smooth Tubes and channels, Int. J. Heat Mass Transfer, Vol.16, pp.347-358,
- Clark, N.N. and Dabolt, R.J., A (1986), general design equation for air lift pumps operating in slug flow. AIChE Journal, Vol. 32, No. 1, pp. 56-64,.
- Collier, J. G., and Thome, J. R., (1996), Convective Boiling and Condensation, McGraw-Hill Book Co., New York,.
- de Cachard, F. and Delhay, J.M., (1996), A slug-churn model for small-diameter airlift pumps, Int. J. Multiphase Flow, Vol. 22, No. 4, pp. 627-649,.
- Delano, A.D., (1998), Design Analysis of the Einstein Refrigeration Cycle, PhD Dissertation, Georgia Institute of Technology.
- El-Wakil, M.M., (1979), Nuclear Power Engineering, McGraw-Hill, New York, N.Y.,.
- Kouremenos, D.A. and Staicos, J., (1985), Performance of a small air-lift pump, Int. J. Heat Fluid Flow, Vol. 6, pp. 217-222,.
- Reinemann, D.J., Parlange, J.Y., and Timmons, M.B., (1990), Theory of small-diameter airlift pumps, Int. J. Multiphase Flow, Vol. 16, pp. 113-122,.
- Saleh, M. M., (2000), Basic Design Report for A Domestic Absorption Refrigeration Cycle, Ibn-Unis Center Eng. Design,.
- Stenning, A. and Martin, C., (1968), An analytical and experimental study of air-lift pump performance, ASME Journal of Engineering for Power, pp. 106-110,.
- White, S. J., (2001), Bubble Pump Design and Performance, M. Sc. Thesis, Georgia Institute of Technology.

NOMENCLATURE

- B_o Bond number = $\frac{(\rho_l - \rho_v)gD^2}{\sigma}$
- C_L Concentration of ammonia in aqua ammonia liquid, $\frac{kg \text{ ammonia}}{kg \text{ liquid}}$
- C_v Vapor composition, $\frac{kg \text{ ammonia vapor}}{kg \text{ vapor mixture}}$
- D Diameter, m
- f Darcy friction factor = $4 * f_{Fanning}$
- G Mass flux, kg/m^2s



g	Gravitational acceleration=9.81 m/s ²
H	Strong solution level, m
h	Enthalpy, kJ/kg
j	Superficial velocity, m/s
\dot{m}	Mass flow rate, kg/s
P	Pressure, pa
q	Heat input, J/s
S	slip ratio
T	Temperature, degree Celsius
V	Velocity, m/s
x	Quality

GREEK SYMBOLS

α	Void fraction
Γ	Parameter in Chisholm's friction pressure drop, Equation 11
ρ	Density, kg/s
σ	Surface tension, N/m
ϕ_m^2	Martinelli-Nelson friction pressure drop multiplier, equation 10
φ	Two phase factor = $\frac{\rho_V}{\rho_L} S$

SUBSCRIPTS

a	Acceleration
B	Boiling
c	Contraction
d	Driving (pressure)
e	Exit or Expansion
f	Friction
in	Inlet
L	Liquid
mn	Minor losses
TP	Two phase
V	Vapor